JOURNAL OF BACTERIOLOGY, June 2006, p. 3837–3848 Vol. 188, No. 11
0021-9193/06/$08.00+0 doi:10.1128/JB.00239-06

The Superoxide Dismutases of *Bacillus anthracis* Do Not Cooperatively Protect against Endogenous Superoxide Stress

Karla D. Passalacqua,[1] Nicholas H. Bergman,[1,2] Amy Herring-Palmer,[1] and Philip Hanna[1]*

Department of Microbiology and Immunology[1] and Bioinformatics Program,[2]
University of Michigan Medical School, Ann Arbor, Michigan 48109

Received 15 February 2006/Accepted 13 March 2006

The *Bacillus anthracis* chromosome encodes four unique, putative superoxide dismutase (*sod*) genes. During exponential growth and sporulation, *sodA1*, *sodA2*, and *sodC* are transcribed constitutively throughout the growth cycle as individual genes. In contrast, the transcription of *sod15* occurs mainly during late exponential and sporulation phases as part of a four-gene operon that may be involved in spore formation. Vegetative cell and spore lysates of wild-type Sterne and superoxide dismutase deletion (Δ*sod*) mutants show detectable SOD activity for SODA1 and SODA2, and protein analysis suggests that these two proteins form active homodimers and heterodimers. A comparison of the growth of parental versus Δ*sod* mutants under various chemical oxidative stresses indicates that Δ*sodA1* mutants are particularly sensitive to endogenously produced superoxide, whereas Δ*sodA2*, Δ*sod15*, and Δ*sodC* mutants remain as resistant to this stress as the parental strain. In addition, in mouse survival assays, Δ*sod15* and Δ*sodA1* were responsible for less end-point death, but the level of decreased virulence does not fall within a statistically significant range. Collectively, these data show that *sodA1* acts as a major protectant from intracellular superoxide stress, that *sod15* is transcribed as part of an operon that may play a role in cell morphology, and that *sodA2* and *sodC* may have minor roles that are not apparent in the conditions tested here.

The plasmid-encoded virulence factors (toxin and capsule) of the endospore-forming bacterium *Bacillus anthracis*, the causative agent of the disease anthrax, have been studied extensively (11, 46). However, the functions of the approximately 5,500 chromosomally encoded genes in this pathogen's biology and disease-causing capability are now beginning to be explored (8). The genome of *B. anthracis* has the potential for a high level of redundancy; for example, there are four phospholipases, five catalases, four superoxide dismutases, etc. By utilizing multiple genes in a modular fashion, bacteria are able to adjust quickly to various environmental stresses and insults, such as heat, changes in osmolarity, nutrient and metabolite deprivation, and highly oxidative conditions (54). This adaptability is of particular importance to pathogens, since they face multiple stresses within a host. *B. anthracis* responds to inhospitable conditions in the soil by forming dormant, metabolically inert endospores. The endospore is the form of the bacterium that can enter a mammalian host via various routes (respiratory, cutaneous, or gastrointestinal) and cause the disease anthrax. Once inside the host, the spores germinate and outgrow, effectively transforming into a replicative, metabolically active vegetative form. The pathogenesis of this microorganism is particularly complex since it is marked by two unique forms of the bacterium, a transition from one form to the other, and a spatial and temporal shift from one locale (the lung, skin, or gastrointestinal tract) to another (regional lymph nodes and the circulatory system) (10, 20).

B. anthracis is a facultatively aerobic organism and so, like all aerobes, must protect itself from toxic forms of oxygen that are produced during normal metabolism. Various antioxidant enzymes (superoxide dismutases, catalases, and peroxidases) and radical-neutralizing metabolites are the main mechanisms by which oxygen-utilizing organisms protect themselves from oxidative damage (3, 55). Pathogens must protect themselves from additional oxidative insults within a host environment, such as the oxidative burst of professional phagocytic cells and the varying oxidative environments within cellular and extracellular compartments. Although the phagocytic oxidative burst is known to be an important bactericidal weapon of the immune system (24, 42), the exact mechanism by which it works is still unclear and a subject of debate (49, 50). In addition, the role that self-generated reactive metabolites play in prokaryotic cellular regulation is also now beginning to be addressed (22).

Superoxide dismutase (SOD) proteins were discovered and characterized by McCord and Fridovich in the 1960s (36). There are two main classes of SOD proteins differentiated by their metal specificity: Mn or Fe versus Cu-Zn. It was at first thought that only eukaryotic species utilized Cu-Zn SODs, but it has since been shown that Cu-Zn SODs are quite ubiquitous in the prokaryotic world (30). SOD enzymes are highly conserved and exist in almost all aerobic organisms studied and even in many strict anaerobes (6). All SODs perform one chemical reaction: the dismutation of superoxide anion ($O_2^{\cdot -}$), the first reduction product of molecular oxygen, to hydrogen peroxide (H_2O_2) and molecular oxygen. By catalyzing this reaction, SODs act as scavengers of $O_2^{\cdot -}$, which can cause direct cellular damage or lead to the formation of other more reactive species such as hydroxyl radical or peroxynitrite (26). Both classes of SODs have been identified in many bacterial species. In some, such as *Salmonella enterica* serovar Typhimurium,

* Corresponding author. Mailing address: Department of Microbiology and Immunology, University of Michigan Medical School, 1150 West Medical Center Dr., 6703 Medical Science Building II, Ann Arbor, MI 48109. Phone: (734) 615-3706. Fax: (734) 764-3562. E-mail: pchanna@umich.edu.

TABLE 1. Bacterial strains and plasmids used in this study[a]

Strain or plasmid	Relevant phenotype	Source or reference
Strains		
Bacillus anthracis		
Sterne $34F_2$	$pXO1^+$, $pXO2^-$	Sterne (1937)
KDC1	$34F_2$ Δ*sod15*::Km^r	This study
KDC2	$34F_2$ Δ*sodC*::Km^r	This study
KDC3	$34F_2$ Δ*sodA1*::Km^r	This study
KDC4	$34F_2$ Δ*sodA2*::Km^r	This study
KDCom3	$34F_2$ Δ*sodA1*::Km^r, pBJ258(*sodA1*::Erm^r)	This study
KDCom4	$34F_2$ Δ*sodA2*::Km^r, pBJ258(*sodA2*::Erm^r)	This study
Escherichia coli		
DH5α	F^- ϕ80*lacZ*ΔM15 Δ(*lacZYA-argF*)*U169 recA1 endA1 hsdR17*(r_K^- m_K^+) *phoA supE44 thi-1 gyrA96 relA1* λ^-	Invitrogen
XL1-Blue	*recA1 endA1 gyrA96 thi-1 hsdR17 supE44 relA1 lac* [F′ *proAB* $lacI^qZ$ΔM15 Tn*10* (Tet^r)]	Stratagene
One Shot TOP10	F^- *mcrA* Δ(*mrr-hsdRMS-mcrBC*) ϕ80*lacZ*ΔM15 Δ*lacX74 recA1 araD139* Δ[ρ](*ara-leu*)*7697 galU galK rpsL* (Str^r) *endA1 nupG*	Invitrogen
CGSC 6478	GM272 (*dam-3*, *dcm-6*)	Palmer and Marinus (1994)
INV110	F′ (*tra*Δ *36 proAB* $lacI^q$ *lacZ*Δ[ρ]M15) *rpsL* (Str^r) *thr leu endA thi-1 lacY galK galT ara tonA tsx dam dcm supE44* Δ[ρ](*lac-proAB*) Δ(*mcrC-mrr*)*102*::Tn*10*(Tet^r)	Invitrogen
Plasmids		
pGEM-T Easy	Amp^r	Promega
pKSV7	pUC_{ori} $pE194_{ori(ts)}$$ap^rcm^r$	52
pDG783	pSB118::Km^r	21
pBJ258	Erm^r	Brian Janes

[a] Strains created for this study were made utilizing the TIGR Comprehensive Microbial Resources Genome sequence for the virulent *Bacillus anthracis* Ames strain since the Sterne $34F_2$ genome sequence was not available at the time this study was started. Therefore, BA numbers referenced in this study are from the Ames sequence; however, the sequences of all four *sod* genes are 100% identical in Sterne $34F_2$ and Ames. Amp^r, ampicillin resistance; Km^r, kanamycin resistance; Erm^r, erythromycin resistance; Tet^r, tetracycline resistance.

SODs have been implicated in the pathogen's ability to cause disease (15, 16, 59). The case of *Mycobacterium tuberculosis* is more complex, with conflicting data about which SOD, the Cu-Zn or the Fe form, is more important to the disease-causing ability of this important pathogen (5, 12, 14, 41). SODs have also been implicated as being important for virulence in *Shigella flexneri* (18) and *Streptococcus agalactiae* (44).

Previously, a proteomic study of the *B. anthracis* endospore showed that two of the four genomically encoded *sod*'s of *B. anthracis*, SODA1 and SOD15, are resident proteins of the endospore (33), the infectious form of the microorganism. Because of this and because *B. anthracis* encodes both classes of SODs, we used a genetic approach to determine whether either of the resident spore SODs (SOD15 and SODA1) or the nonresident SODC and SODA2 proteins are important for the survival of *B. anthracis* during normal growth, growth under oxidative stress, and growth during infection of mice.

MATERIALS AND METHODS

Plasmid and bacterial strain construction. Strains and plasmids used in the present study are listed in Table 1. The creation of Δ*sod* mutants was performed as follows. Oligonucleotide primers (Invitrogen) for PCR amplification of SOD genes (all primer sequences available upon request) were designed by using the *Bacillus anthracis* Ames strain genomic sequence from the TIGR Comprehensive Microbial Resource and Manatee Server. All initial cloning strategies were facilitated with the use of the *Escherichia coli* strains listed in Table 1. The strategy was as follows. The SOD genomic regions were PCR amplified with either Sigma Klen*Taq* or Invitrogen Platinum *Taq* high-fidelity systems using *B. anthracis* Sterne strain $34F_2$ genomic DNA with a 5′ BamHI restriction site and a 3′ KpnI restriction site. These fragments were ligated into the Promega pGEM-T Easy vector and selected for by *lacZ* selection on LB-ampicillin plates. "Inside-out PCR" was then performed (all primers are available upon request) creating XhoI and XbaI restriction sites such that 292 to 354 bp were omitted from the wild-type sequence. A kanamycin resistance cassette PCR amplified from vector pDG783 (21) with XhoI and XbaI restriction sites was ligated into these fragments and transformed for passage in *E. coli* DH5α or XL1-Blue. Standard minipreps (QIAGEN) were used to isolate plasmid, and the entire construct was PCR amplified and digested for insertion into recombination vector pKSV7 (52) by standard techniques utilizing Invitrogen T4 DNA ligase. pKSV7 constructs were passaged through dam^+ dcm^+ and *dam dcm* strains listed in Table 1. Transformation of pKSV7::Δ*sod* plasmids into *Bacillus anthracis* Sterne $34F_2$ was done according to methods described previously (45) with the following modification: cells were allowed to recover after electroporation for 1 to 4 h in brain heart infusion (BHI) broth at 30°C with no shaking. Allelic exchange was performed as follows. After electroporation and recovery, cells were plated on BHI-kanamycin plates and grown at 30°C overnight to 2 days. Colonies were picked, grown in BHI-kanamycin broth at the nonpermissive temperature of 39.5°C, shaken at 300 rpm, and back-diluted 1:1,000 five to seven times to facilitate plasmid integration. These cultures were then shifted to the permissive temperature of 30°C in BHI broth with no antibiotic to facilitate allelic exchange. These cultures were back-diluted 1:1,000 every 12 h eight to eleven times. The cultures were then shifted to the nonpermissive temperature of 39.5°C to facilitate clearance of any cytoplasmic plasmid and back-diluted 1:1,000 every 12 h eight to eleven times. Cultures were streaked onto BHI plates and patch plated to screen for loss of chloramphenicol resistance and gain of kanamycin resistance. Candidate transformants were verified by Southern blotting and/or multiple PCRs. All strains were screened by PCR for the presence of the pXO1 plasmid.

All strains were sporulated as follows. Briefly, overnight BHI broth cultures (<12 h old) were diluted 1:20 into modified G medium and shaken at 30°C at 300 rpm for 3 days. The cultures were pelleted by centrifugation at 3,000 rpm for 30 min and washed five times in 45 ml of sterile Milli-Q water. The cultures were heat treated at 65°C for 30 min to kill any remaining vegetative bacilli and then pelleted by centrifugation once more and transferred into 1.5-ml volume screw-

cap tubes in 1-ml volumes of sterile Milli-Q water. The cultures were then pelleted by centrifugation and washed two to three times with sterile Milli-Q water and stored at room temperature. The purity of the spore preparations was confirmed by phase-contrast microscopy, and concentrations were determined by serial dilution.

The antibiotic concentrations were as follows: kanamycin (30 to 50 μg/ml), chloramphenicol (30 μg/ml [*E. coli*] and 7 to 10 μg/ml [*B. anthracis*]), ampicillin (100 μg/ml), and erythromycin (300 to 400 μg/ml [*E. coli*] and 5 μg/ml [*B. anthracis*]).

***B. anthracis* growth under oxidative and nonoxidative conditions.** Cultures of *B. anthracis* Sterne strain ($34F_2$) and Δ*sod* mutant strains ($34F_2$ parental strain) were grown overnight in LB broth or LB plus selective antibiotic for less than 12 h. In the morning, cultures were diluted into fresh LB broth to an optical density at 600 nm (OD_{600}) of 0.1 to 0.2 and allowed to recover for 1.0 to 1.5 h at 37°C with shaking at 300 rpm. These cultures were then diluted and adjusted to an OD_{600} of 0.01 in fresh LB or LB plus selective antibiotic in a final volume of 50 or 70 ml and then shaken at 250 rpm at 37°C. OD_{600} was measured at 1-h intervals. For growth curves testing sensitivity to oxidative stress, redox cycling reagents were added when cultures reached exponential growth (OD_{600} = 0.4 to 0.6), usually at time point 2.5 h. A flask with water added instead of paraquat served as a growth control. Paraquat at 194 mM (Ultra Scientific PST-740) was added to a final concentration of 300 or 800 μM. Growth curves were determined three times on separate days utilizing three unique spore stocks of each strain.

Disk diffusion assays of tolerance to redox cycling compounds. Cultures of *B. anthracis* Sterne strain ($34F_2$) and Δ*sod* mutant strains ($34F_2$ parental strain) were started from a colony grown on BHI agar plates in BHI medium or BHI medium plus selective antibiotic. Cells were grown at 37°C shaking at 300 rpm to an OD_{600} of 0.4 to 0.5. Plate assays were performed by adding 200 μl of mid-log-phase cultures to 2 ml of 0.7% sterile soft agar. Then, 3 ml of the agar suspensions was spread onto BHI plates. Sterile paper disks (6 mm in diameter) were permeated with 10 μl of either 5% paraquat (Ultra Scientific PST-740 or Sigma methyl viologen M-2254), 0.08 M menadione (Sigma M5625) dissolved in ethanol, or 66 mM plumbagin (Sigma P7262) dissolved in ethanol or distilled water (negative control). Disks were placed on plates and incubated overnight at 37°C. Zones of inhibition were measured in millimeters. For each experiment, 10 disks (2 disks per plate) were used.

Change in OD_{600} germination assay. Spores of *B. anthracis* Sterne ($34F_2$) or Δ*sod* mutant strains ($34F_2$ parental strain) were placed in a microcuvette (Bio-Rad 22309955) to an OD_{600} 0.3. in 1 ml of germination buffer (100 mM phosphate-buffered saline [PBS] plus 100 mM L-alanine). The change in the OD_{600} was measured every 60 s for 20 min using the kinetic read function on a Beckman DU530 spectrophotometer. The percent fall in the OD was calculated as follows: $\{[OD_{600}(\text{time zero}) - OD_{600}(\text{time 20 min})]/OD_{600}(\text{time zero})\} \times 100$. As shown previously, a decrease in the OD of ~60% correlates to loss of heat resistance in >99% of cultures (17). Experiments were performed with at least three different spore preparations.

Nondenaturing polyacrylamide gel electrophoresis (PAGE) assay of SOD activity. *B. anthracis* Sterne strain ($34F_2$) and Δ*sod* mutants ($34F_2$ parental strain) were grown in modified G medium to late exponential phase (OD_{600} of ~0.9). Portions (6 ml) of cultures or 200 μl of purified spore preps were pelleted at 4°C, washed twice in cold PBS, and resuspended in 1 ml of 0.05 M potassium phosphate buffer (pH 8.0) plus 25 mM benzamidine. Suspensions were transferred to 2.0-ml screw-cap tubes filled halfway with acid-washed glass beads (diameter, 150 to 200 μm; Sigma G-1145). Cells were disrupted mechanically via bead beating with a Biospec mini-bead beater on high speed 10 times for 1 min with at least a 5-min rest on ice between pulses. Tubes were spun at 4°C for 10 min at 1,000 rpm. Supernatants were transferred to fresh tubes and spun at 4°C for 10 min at 1,000 rpm. Then, 2 μl of DNase I, RNase-free (Roche), was added, followed by incubation on ice for 1 h and spinning at 5,000 rpm for 10 min at 4°C. Supernatants were transferred to a new tube and centrifuged at 14,000 rpm for 30 to 40 min. Supernatants were quantified for soluble protein by using the Bio-Rad protein assay. A total of 25 μl (ca. 30 to 80 μg of protein) was run on an Invitrogen 12% pre-cast Tris-glycine gel in Invitrogen nondenaturing Tris-glycine buffer. After electrophoresis, the gel was soaked in 0.05 M potassium phosphate buffer (pH 8.0) plus 50 mM EDTA plus 2 ml of 20 mg of nitroblue tetrazolium (NBT; Sigma N-5514)/ml and 6 ml of 0.5 mM riboflavin for 20 min. Gels were developed for 15 min under a miniature UV lamp.

Cell growth conditions and RNA isolation. For quantitative reverse transcription-PCR (RT-PCR) of *sod* expression during sporulation, overnight BHI broth cultures of *B. anthracis* Sterne strain ($34F_2$) were diluted 1:1,000 in the morning into nutrient-limiting (sporulation) modified G medium. Cells were harvested at an OD_{600} of 0.4 to 0.5, 0.7, 0.8, 0.9, and 1.1. Portions (5 to 7 ml) of cultures were collected and pelleted by centrifugation at 4°C. For end-point RT-PCR to determine transcriptional products of the *sod15* operon, *B. anthracis* Sterne ($34F_2$) and the Δ*sod15* strain were grown similarly but harvested at an OD_{600} of 0.9 to 1.0. RNA isolation was performed by using the Ambion RiboPure-bacteria kit according to the manufacturer's instructions with the following modifications: cell disruption with zirconia beads was done for 15 min, 400 μl of RNAwiz reagent was used, BCP phase separation reagent was used in place of chloroform, and 50 μl of RNase/DNase-free distilled water was added during extraction. The QIAGEN RNEasy mini-kit with a DNase digestion step was used according to the manufacturer's RNA cleanup protocol. RNA was quantitated via the A_{260}/A_{280} ratio on a Beckman DU530 spectrophotometer. Then, 1 μg of RNA was run on a denaturing formaldehyde gel to verify the RNA integrity. These procedures were carried out in three separate experiments utilizing unique cultures each time.

SYBR green quantitative RT-PCR. For quantitative RT-PCR, RNA was collected as described above, and cDNA was made from RNA samples utilizing Invitrogen random primers and Invitrogen SuperScript II reverse transcriptase. Briefly, random primers were used at 300 ng/μl with 1 μg of RNA and incubated overnight at 42°C. All samples were also run with no reverse transcriptase. A control PCR was performed on all cDNA samples to verify no genomic DNA contamination. Then, 1.5 μl of each cDNA reaction was used in 20-μl PCRs using an Applied Biosystems SYBR green master mix. Each sample was run twice in a full reaction: once with no cDNA and once with cDNA made with no RT. Reactions were run in a 384-well plate at the University of Michigan Comprehensive Cancer Center cDNA core facility on an ABI Prism 7900 HT SDS with the SDS Software version 2.0 sequence detection system using an annealing temperature of 56.4°C and an extension at 72°C for 1 min with 35 cycles. All primers were sequence specific for each gene analyzed, with PCR products of between 171 and 191 bp. The mean of the C_T (threshold cycle) values for the duplicate runs and triplicate biological samples were used.

Endpoint RT-PCR. A total of 750 ng of RNA collected from *B. anthracis* Sterne $34F_2$ grown as explained above was used to perform endpoint RT-PCR using Invitrogen one-step RT-PCR with Platinum *Taq* according to the manufacturer's instructions. Briefly, RT was performed at 50°C for 30 min. PCR was performed with 0.25 pg of operon/gene-specific primers (the sequences are available upon request) for 35 or 37 cycles with an elongation temperature of 70°C and an extension time of 1 min and 10 s. Next, 5 μl of endpoint PCR product was run on 0.7% agarose gels and visualized by ethidium bromide staining. Negative controls omitting reverse transcriptase and positive controls with *B. anthracis* Sterne ($34F_2$) genomic DNA were done with each experiment. Operon/gene-specific primers were designed to result in 0.6- to 1.0-kb products.

Transmission electron microscopy. *B. anthracis* spores or vegetative bacilli were fixed in 2.5% glutaraldehyde in 0.1 M Sorensen buffer (pH 7.4) overnight at 4°C. After several buffer rinses, the spores were postfixed in 1% osmium tetroxide in the same buffer. They were then rinsed in double-distilled water to remove phosphate and then stained en bloc with aqueous 3% uranyl acetate for 1 h. They were dehydrated in ascending concentrations of ethanol, treated with propylene oxide, and embedded in Spurr's epoxy resin over the course of 7 days. Ultrathin sections, 70 nm in thickness, were poststained with uranyl acetate and lead citrate. Sections were then examined by using a Philips CM100 electron microscope at 60 or 80 kV. Images were recorded digitally using a Hamamatsu ORCA-HR digital camera system operated using AMT software (Advanced Microscopy Techniques Corp., Danvers, MA).

Determination of primary protein sequence distances. The DNASTAR Lasergene v6 program MegAlign was used for determining the protein sequence identities and divergence. Multiple alignments were performed by using the CLUSTAL W method set on a "slow-accurate" parameter with a gap penalty of 10.00. MegAlign calculates the divergence between sequences by comparing sequence pairs in relation to a reconstructed phylogeny that is generated by the program. It should be noted that the percent identity is a direct comparison, but divergence is calculated by comparing sequence pairs to a phylogeny reconstructed by the program used and so is not an inverse of percent identity (i.e., this number can be >100).

Infection of DBA/2 mice with *B. anthracis* Sterne and Δ*sod* spores. Intratracheal infection of mice. Briefly, mice were anesthetized with ketamine-xylazine, and a small incision was made through the skin above the trachea. A 30-μl inoculum containing approximately 100, 1,000, 10,000, or 100,000 spores suspended in water was delivered to the lung with a 30-gauge needle plus a 1-ml syringe. Spores were quantitated pre- and postinfection via serial dilutions on BHI plates. Postmortem necropsies were performed, and *B. anthracis* strains were isolated on BHI or BHI-kanamycin plates from lung and/or spleen homogenates of all terminal animals and on one surviving animal of each group at the end of the experiments. Mice were monitored three times a day for morbidity and mortality for 10 days. The 50% lethal dose (LD_{50}) was calculated by the

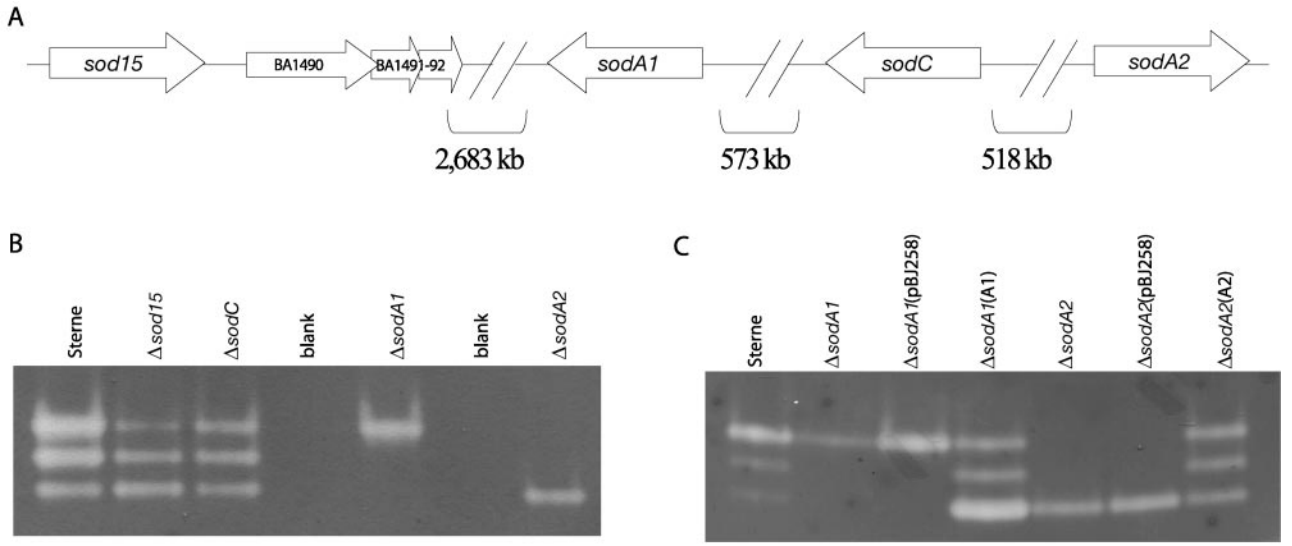

FIG. 1. Genomic location of *B. anthracis* SOD genes (*sod*) and SOD activity assay. (A) Distribution of the four putative SOD (*sod*) open reading frames on the *B. anthracis* Ames genome (BA1489, BA5139, BA4499, and BA5696, respectively) and the sizes of the intergenic spaces. (B and C) SOD activity on native PAGE-nitroblue tetrazolium gels from vegetative cell lysates of Sterne and Δ*sod* mutants (B) and vegetative cell lysates of complementation strains for *sodA1* and *sodA2* (C).

method of Reed and Muench (48). For each dose of spores, the total number of mice utilized was as follows: (i) 10^2 spores, $n = 4$ for all strains; (ii) 10^3 spores, $n = 9$ mice for all strains except Δ*sodC*, where $n = 4$; and (iii) 10^4 spores, $n = 9$ for Sterne, Δ*sod15*, and Δ*sodA2*, $n = 4$ for Δ*sodC*, and $n = 18$ for Δ*sodA1*. Information regarding the log-rank test may be found online (http://bioinf.wehi.edu.au/software/russell/logrank/).

RESULTS

Bioinformatics of the four *B. anthracis* SOD genes. The *B. anthracis* genome encodes four distinct proteins with conserved SOD domains (Fig. 1A), one of likely Cu-Zn specificity (BA5139 [*sodC*]), two that are putatively manganese (BA4499 [*sodA1*] and BA5696 [*sodA2*]), and one of unknown metal specificity (BA1489 [*sod15*]) (47). As of January 2006, nine different strains of *B. anthracis* are contained in the TIGR Comprehensive Microbial Resource (www.tigr.org/tigr-scripts/CMR2/CMRHomePage.spl), including virulent strains and the attenuated Sterne strain. Although the location of the four *sod* genes displayed in Fig. 1A was derived from the virulent Ames Ancestor strain, the *sod*'s of the toxin-producing, unencapsulated Sterne strain (utilized in the present study) are 100% identical at the nucleotide level and are located on the chromosome in the same regions. The four *sod*'s are located quite far from each other, with two on the leading strand (*sod15* and *sodA2*) and two on the lagging strand (*sodA1* and *sodC*) and no apparent linkages between them. The nomenclature for *sod15* was coined for the present study to underscore its unknown metal specificity and to differentiate it from the other paralogous *sod*'s A1 and A2.

The Mn-containing SODA of *B. subtilis* has been characterized (7, 27), as have the Cu-Zn SODs of *Salmonella* serovar Typhimurium and *M. tuberculosis* (9, 15, 53). Multiple protein alignments were constructed to ascertain the level of primary amino acid sequence conservation that exists between the two classes of these proteins (see Materials and Methods) comparing the following primary amino acid sequences: (i) the three *B. anthracis* Mn-SODs (SODA1, SODA2, and SOD15) with *B. subtilis* SODA and (ii) *B. anthracis* SODC with the Cu-Zn SODs of the two bacterial pathogens *Mycobacterium tuberculosis* and *Salmonella enterica* serovar Typhimurium.

Of the three putatively Mn-containing SODs of *B. anthracis*, SODA1 is the one most closely related to *B. subtilis* SODA with 76.7% identity, while SODA2 maintains a lower identity at 55.4%. Because SODA of *B. subtilis* is the only active SOD seen during all stages of growth and this enzyme is essential for resistance to superoxide in *B. subtilis* (7), this suggested to us that either SODA1 or SODA2, or both, would most likely play the normal role of an antioxidant protectant during aerobic growth or under oxidative stress. SOD15 has only a 36.5% identity with the *B. subtilis* ortholog and is almost completely divergent from the other two *B. anthracis* Mn-SOD paralogs (>100% divergent from SODA1 and SODA2). This degree of divergence is mainly due to an additional N-terminal 135 amino acids encoded in the *B. anthracis sod15* gene. The predicted molecular mass of SOD15 is approximately 36 kDa, which is substantially larger than the average size of most SODs (~23 kDa). SOD15 has identical homologs only in the other pathogenic *Bacillus* species, *B. cereus* and *B. thuringiensis*, suggesting that this particular SOD may have evolved a unique function in these species.

Cu-Zn SODs represent an entirely different class of enzyme from the Mn- or Fe-chelating class of proteins and are present in many bacteria, often periplasmically located in gram-negative species (30, 37, 53). *B. anthracis* encodes one putative Cu-Zn SOD (SODC), and this gene is conserved in the pathogenic *B. cereus* group. We compared the primary sequence of *B. anthracis* SODC to the Cu-Zn SOD of two pathogens, *M. tuberculosis* and *S. enterica* serovar Typhimurium, that are capable of surviving intracellularly, as has been shown for *B. anthracis* (51). The role of SODC in *M. tuberculosis* is unclear,

but it has been shown to possibly play a role in intracellular survival (12, 41), and the *B. anthracis* SODC shares a very low identity at with it at only 21.2%. In *S. enterica* serovar Typhimurium, all strains encode a Cu-Zn enzyme called SODCII, but only highly virulent *Salmonella* species contain an additional phage-encoded Cu-Zn SOD, named SODCI (15). In our CLUSTAL W analysis, the two serovar Typhimurium enzymes share ~58% identity with each other, but neither one is particularly similar to the SODC of *B. anthracis*, which only shares 25% identity with each. Oddly, the Cu-Zn SODs of prokaryotes tend to be very divergent, often lacking obvious metal ligands entirely (1), which is contrary to the high level of conservation in eukaryotic Cu-Zn SODs. The high level of divergence between the *B. anthracis* SODC and the enzymes of serovar Typhimurium and *M. tuberculosis* suggested to us that this putative SOD might play a novel, perhaps specialized, role in the biology of *B. anthracis* or, conversely, might be a relic with no overt physiological role at all.

Since the *B. anthracis* SODs differ considerably from one another and from those in other bacterial species, we hypothesized that these enzymes might play unique roles during different phases of growth and in different growth environments. In addition, proteomic analysis of the *B. anthracis* spore revealed that SOD15 and SODA1 are resident members of the spore, the infectious form of the microbe (33), further suggesting that these SODs may be important during pathogenesis.

Superoxide scavenging by *B. anthracis* SODs from cell lysates. In order to reveal which SOD(s) might be the main superoxide scavenging enzyme of *B. anthracis* and to determine whether any of the four proteins is important for the establishment of the disease anthrax, single-deletion mutants in each of the four *sod* genes were generated. Single-deletion strains were created via homologous recombination involving the removal of approximately 300 nucleotides from each *sod* open reading frame and the insertion of a kanamycin resistance cassette (*sod*::Km^r mutants, hereafter referred to as Δ*sod* mutants). Mutants were then assayed for defects in normal growth, for growth under various oxidative stresses, and for the ability to generate disease in susceptible mice.

Since the enzymatic function of SODs is to scavenge superoxide, we set out to determine whether each of the four *B. anthracis* SODs is present in active form in spore and vegetative cell lysates. To determine which form(s) of the proteins are present in whole bacterial cells, we performed a nondenaturing PAGE-SOD activity assay with cell lysates prepared by mechanical disruption of *B. anthracis* cells (Fig. 1B and C). Three distinct bands of SOD activity can be detected in the wild-type Sterne strain, as well as in the two single deletion mutants Δ*sod15* and Δ*sodC* for both vegetative cells (Fig. 1B) and spores (not shown). However, both the Δ*sodA1* and the Δ*sodA2* mutant display only one band of SOD activity each; the highest band in the former and the lowest band in the latter (Fig. 1B). Complementing Δ*sodA1* and Δ*sodA2* in *trans* with a plasmid-borne copy of the wild-type gene leads to a restoration of the two missing bands for each strain (Fig. 1C). This not only implies that the bands of activity are due to SODA1 and SODA2 homodimers but also strongly suggests that SODA1 and SODA2 form an active heterodimer. Although the uppermost band of activity, which is most likely SODA2, in Fig. 1B for Sterne cells appears to display a qualitatively stronger band of SOD activity, it should be mentioned that this assay is only semiquantitative and that from gel to gel the intensities of each band varied with no apparent pattern. In addition, we believe that the SODA2 bands of activity that we detected from spore lysates are, indeed, from proteins resident in the spore and not from vegetative detritus in the spore preparation, since it seems unlikely that a sufficient amount of nonspore enzyme would be abundant enough to show a clear band of activity.

Iron- and manganese-containing SODs have very similar tertiary structures, and it is sometimes possible to distinguish the two from their primary structures (39, 40). However, anomalies exist, and it is not always possible to distinguish these types of enzymes from specific metal-chelating residues alone (28). Recently, the crystal structures of *B. anthracis* SODA1 and SODA2 were determined (4). In that study, the recombinant proteins were chelated with Mn, the structures determined were homodimers, and the same nondenaturing gel assay was used to confirm that the homodimers of each protein were able to scavenge superoxide. However, the possibility that SODA1 and/or SODA2 might be cambialistic (i.e., able to chelate and utilize both Mn and Fe) has not yet been tested. We performed the NBT gel assay under several conditions, but additional bands of SOD activity corresponding to SOD15 and SODC from cell lysates were not found. At this point, it is unclear whether SOD15 and SODC proteins provide SOD activity at all, whether they simply are not abundant enough in the cell to show a signal in this assay, or whether they had been degraded or inactivated during the gathering of lysate.

Expression of *B. anthracis sod*'s during exponential growth and entry into sporulation. A lack of SOD activity for SOD15 and SODC in the previous assay led us to elucidate the general transcriptional pattern of the four *sod* genes to determine their general expression levels. A previous microarray study (33) suggested that *sod15* was differentially expressed upon entry into late exponential phase. Therefore, we used SYBR green quantitative RT-PCR to verify that that each of the four genes is actively transcribed (Fig. 2 and Table 2). The cells were grown in modified G medium, a specialized medium that promotes the formation of a high number of spores upon entry into stationary phase. *sodA1* consistently showed the highest abundance of mRNA compared to the internal control translation elongation factor g (*fusA*) and was transcribed constitutively with a slight decrease in transcript abundance at OD_{600} higher than 0.9. A constitutive pattern of expression was also seen for *sodC* and *sodA2*, but to different levels. Whereas *sodC* showed almost equal transcript abundance with the internal control *fusA*, *sodA2* had a consistently lower expression than both *sodA1* and *sodC*. Only *sod15* revealed a differential pattern of expression in this growth curve (Fig. 2 and Table 2) where the transcript was ~200-fold less abundant than *fusA* at OD_{600} 0.5 with a steadily increasing amount of mRNA coinciding with an increasing OD_{600}. These data indicate that all four *sod*'s are expressed during the growth cycle, albeit to different levels, and suggest a specialized role for *sod15* after entry into stationary phase and/or during the formation of endospores.

***sod15* is part of an operon during late exponential phase, and Δ*sod15* mutant spores show only slight ultrastructural differences relative to parental spores.** Because *sod15* appeared to be differentially expressed during the late exponen-

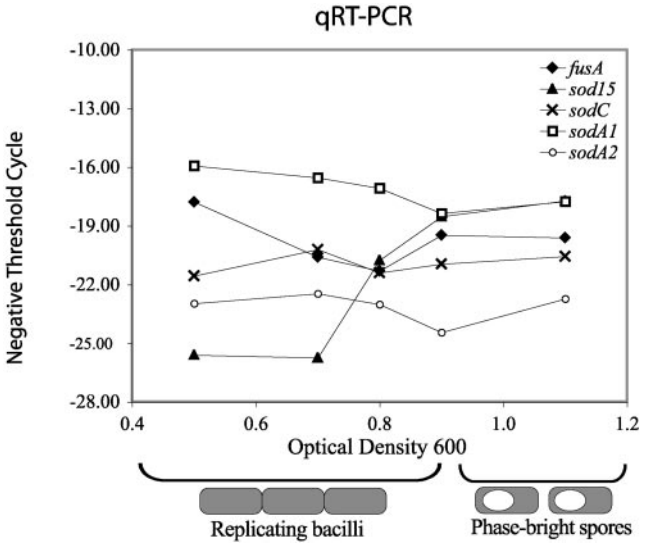

FIG. 2. SYBR green quantitative RT-PCR analysis of *B. anthracis sod* expression during exponential growth and sporulation. Negative threshold cycles (C_T values) listed in Table 2 are plotted to show the pattern of changes in expression levels with increasing OD_{600}, where an OD_{600} of 0.5 represents early to mid-log phase, an OD_{600} of 0.7 to 0.8 represents late log phase, and an OD_{600} of 0.9 to 1.1 represents entry into sporulation phase, where phase-bright spores are visible in the culture. Because lower C_T values are indicative of a higher level of transcript, negative values were used to reflect increases or decreases in mRNA level over time, accordingly.

tial and stationary (sporulation) phases, we looked more closely at the expression of this gene and at the ultrastructure of Δ*sod15* mutant spores. A role for SODs in spore formation has been suggested for *B. subtilis*, where *sodA*-deficient strains form aberrant endospore coats (23). Other genes linked to a similar endospore phenotype in *B. subtilis* include a three-gene operon composed of *dacB* (a D-alanyl-D-alanine carboxypeptidase/penicillin-binding protein) and *spmA* and *spmB* (spore maturation proteins), where these genes appear to be necessary for the formation of heat-resistant spores with a normal ultrastructure (43). In *B. subtilis*, *sodA* and the *dacB* operon are about 161 kb apart from each other. In *B. anthracis*, one of the four putative *sod*s, *sod15*, is located only 116 bp upstream of the *dacB* operon homologs (BA1490-1492; referred to here as $dacB_{Ba}$, *spmA*, and *spm*). This gene order that includes *sod15* is conserved only within the pathogenic *B. cereus* group. Neither the intergenic distance (116 bp) between *sod15* and *dacBBa*, *spmA*, and *spm* (~50, 66, and 66% amino acid identity with *B. subtilis dacB*, *spmA*, and *spmB*, respectively) nor their putative protein functions overtly imply operon-linkage. However, a new operon-prediction algorithm developed by N. H. Bergman and Z. S. Qin (unpublished data) suggested that these four genes might be transcribed as one unit. To determine whether *B. anthracis sod15*, *dacBBa*, *spmA*, and *spm* are transcribed as a single mRNA unit, we performed endpoint RT-PCR from RNA collected from wild-type Sterne and Δ*sod15* cells grown to both a low and a high OD_{600} (0.4 and 1.0, respectively) using various primer sets designed to overlap the four genes (Fig. 3A and B). In both wild-type Sterne cells and Δ*sod15* mutants at an OD_{600} of 0.4, no transcript overlapping *sod15* and *DacBBa* was detected, but transcript within the *sod15* gene in Sterne was seen, suggesting that transcription of these genes during early log phase is separate. The tightly linked three-gene operon of *dacBBa*, *spmA*, and *spm* is seen as a contiguous unit at a low OD_{600}. Interestingly, at an OD_{600} of 1.0, a transcript overlapping all four genes was readily detected in both Sterne and Δ*sod15*. Predictably, no transcript from within the *sod15* gene was detected in the Δ*sod15* mutant. The presence of transcripts overlapping *sod15* and *dacBBa* in both strains but only during late log phase implies the presence of multiple promoters. This indicates that, at least during late exponential phase and entry into stationary phase, the products of these four genes may serve a cooperative function and also suggests that they may be part of a stress-induced regulon.

To determine whether the removal of *sod15* affected endospore ultrastructure, we performed transmission electron microscopy on Sterne ($34F_2$) and Δ*sod15* endospores (preparations were also made for Δ*sodA1* and Δ*sodC* mutants [not shown]). Figure 3C shows micrographs of endospores of both strains at ×64,000 (left two panels) and ×245,000 (right two panels) magnifications. The lower magnification shows no overt differences in the ultrastructure of the spores, and the average size of the spores (900 nm to 1 μm) did not differ between the two strains. An intact exosporium and thick cortex was observed in both strains. At a higher magnification, the spore coat and cortex can be seen in more detail. The spore coat of *B. anthracis* differs markedly from that of *B. subtilis* in thickness, and the protein composition of the endospore coats differs from species to species (31). Sterne spores consistently showed a very clear, double-layered protein coat with a visible outer membrane located between the spore coat and the cortex. Spore coats of the Δ*sod15* mutant typically had a more diffuse, multilayered appearance (Fig. 3C) but by no means revealed the striking phenotype of *B. subtilis sodA* mutants (23). Although it remains formally possible that this appearance is an artifact of thin sectioning, this form of the spore coat was not detected in several preparations of the parental Sterne strain. The Δ*sod15* strain sporulates in modified G medium as efficiently as Sterne, and the spores show only a slight increase in sensitivity to wet heat at 70°C (not shown). In addition,

TABLE 2. SYBR green quantitative RT-PCR of *sod* genes of *B. anthracis* during exponential growth and entry into sporulation[a]

OD_{600}	*fusA*[b] (mean C_T)	*sod15*		*sodC*		*sodA1*		*sodA2*	
		Mean C_T	FD	Mean C_T	FD	Mean C_T	FD	Mean C_T	FD
0.5	17.7	25.6	−200.0	21.6	−15	15.9	+3.5	23.0	−39.4
0.7	20.6	25.7	−34	20.2	+1.3	16.5	+17.1	22.5	−3.7
0.8	21.3	20.7	+1.5	21.4	−1.0	17.1	+18.4	23.0	−3.2
0.9	19.5	18.5	+2	21.0	−1.5	18.4	+2.1	24.5	−32.0
1.1	19.6	17.7	+3.7	20.6	−2.0	17.8	+3.5	22.7	−8.5

[a] SYBR green quantitative RT-PCR is interpreted via C_T values, which are the values at which the PCR reaction crosses a set threshold into exponential phase; therefore, a lower C_T value indicates a more abundant transcript. The fold difference (FD) is as compared to the reference gene "elongation factor g" and was calculated as: C_T higher − C_T lower = x. The lower-value C_T transcript is approximately 2^x times more abundant than the higher C_T transcript.

[b] The translation elongation factor G gene *fusA* (BA0107 or BAS0107) was chosen as a reference since previous microarray data (33) indicate that, during growth and sporulation, transcript levels of this gene are never more than 1× higher or lower than the pooled RNA reference.

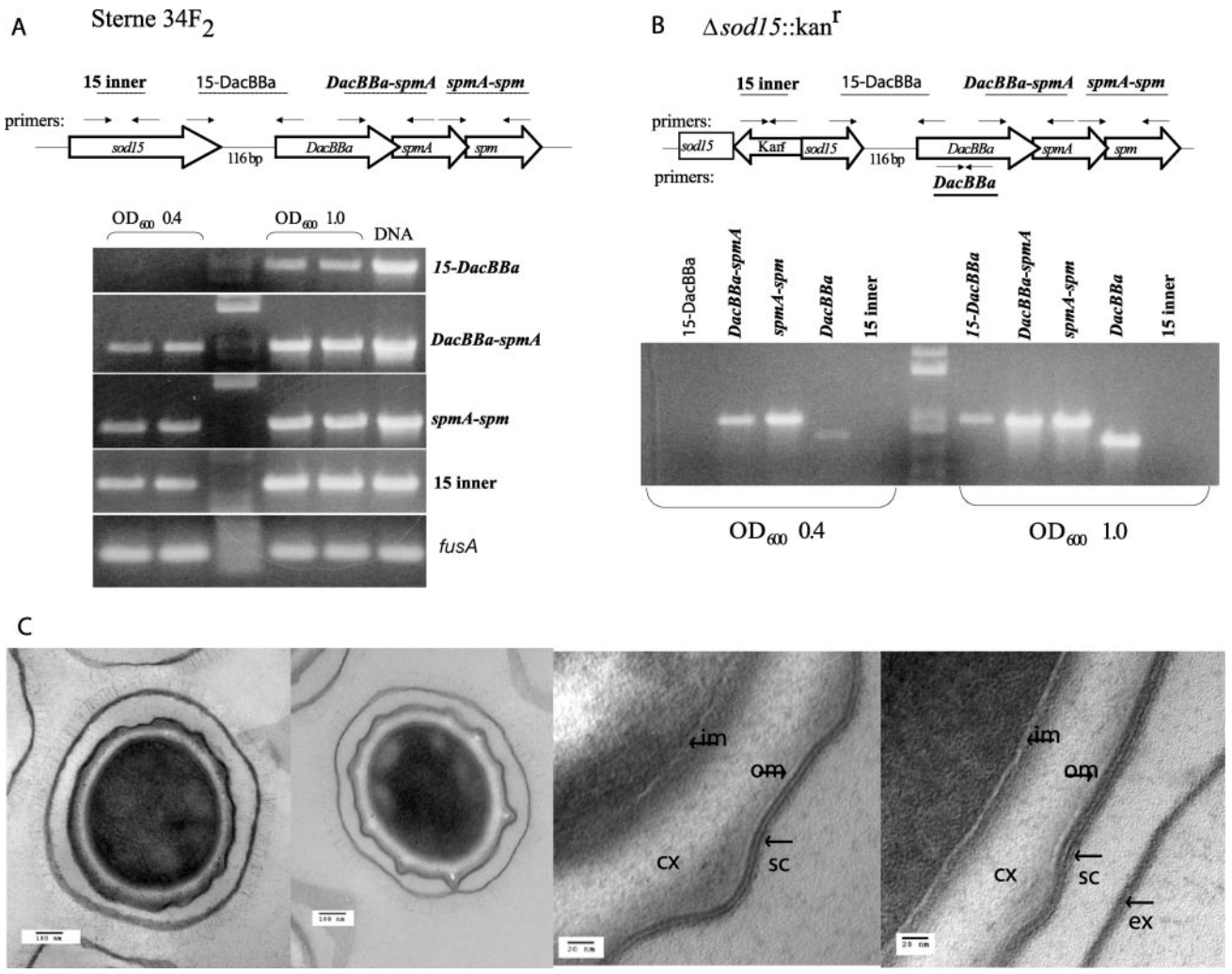

FIG. 3. *sod15* is part of a four-gene operon at high OD_{600}, and Δ*sod15* spores are similar to parental Sterne spores as seen by transmission electron microscopy. Endpoint RT-PCR shows that *sod15* is transcribed as part of a contiguous transcript at high OD_{600}. (A and B) Primers (arrows) and their predicted gene-overlap products (lines) are indicated above and below the open reading frames of the *sod15* (BA1489) and Δ*sod15* genomic regions: D-alanyl-D-carboxypeptidase (*DacBBa* [BA1490]), spore maturation protein A (*spmA* [BA1491]), and spore maturation protein (*spm* [BA1492]). Gels showing contiguous products at low (0.4) and high (1.0) OD_{600}s from the indicated primer pairs. Two lanes on each side of ladder in panel A are biological replicates. Non-reverse-transcriptase-containing negative controls revealed no genomic DNA contamination (not shown). (C) Transmission electron microscopy of Sterne ($34F_2$) and Δ*sod15* whole spores at ×64,000 magnification (left two panels) and details of spore coat structures at ×245,000 magnification (right two panels). cx, cortex; sc, spore coat; ex, exosporium; om, outer membrane; im, inner membrane.

Δ*sod15* germinates identically to the parental Sterne strain as measured by the change in OD_{600} with the addition of the germinant L-alanine (100 mM in PBS) with an average drop in OD_{600} of ca. 53% over the course of 21 min for both strains. The modest changes in the spore structure of the *B. anthracis* Δ*sod15* mutant differ radically from the dramatic phenotypic changes seen in *B. subtilis* by removal of either its *sodA* or the *dacB* operon. We conclude that in the late exponential and stationary phases, there is transcriptional linkage between *B. anthracis sod15* and three downstream genes that have been implicated in spore formation in *B. subtilis*. The obvious controlled expression of *sod15* and its operon linkage strongly suggest that this protein has evolved a novel role in spore formation, but it appears to be less critical than *B. subtilis sodA*. In addition, although a contiguous mRNA unit was detected for the *dacBBa* operon in the Δ*sod15* mutant at both low and high OD_{600} values, it cannot be ruled out that a polar effect has occurred in the more downstream genes, either due to frameshift or to changes in the *dacBBa* promoter. The possible functional relationship between the genes in the *sod15* transcriptional unit remains unclear and is currently under investigation.

SODA1 is responsible for protection from intracellular superoxide. The typical role of SODs in cells is to scavenge superoxide as a first defense in preventing the oxidative damage of biomolecules. Superoxide is a byproduct of electron transport during aerobic growth (26), and although in itself is not a particularly reactive oxygen radical (13), its presence can lead to the release of free iron in the cell from proteins that contain [4Fe-4S] and [2Fe-2S] clusters, which can then, in the

presence of H_2O_2, lead to the formation of the highly reactive hydroxyl radical via the Fenton reaction (25, 29, 57). We tested each single Δ*sod* mutant for sensitivity to compounds that cause the generation of intracellular superoxide radical. In broth growth assays, all Δ*sod* mutants were indistinguishable from wild-type Sterne in rich medium (LB) at 37°C (Fig. 4A). With the addition of the redox cycling compound paraquat added at mid-exponential phase to final concentrations of 300 and 800 μM, only the Δ*sodA1* mutant showed an obvious growth defect (Fig. 4A and B). At 300 μM, Δ*sodA1* leveled off in growth after the addition of paraquat, with all other strains attaining stationary phase equivalently (Fig. 4B). At the higher paraquat concentration of 800 μM, the Δ*sodA1* strain was highly sensitive, leveling off in growth for several hours and then showing a decrease in OD_{600} (Fig. 4C). At this concentration, all other strains, including Sterne, grew to only a slightly lower OD_{600} in the stationary phase than Sterne cells with no treatment. We conclude that in broth growth, under high superoxide stress, the presence of SODA1 is necessary to allow for robust growth.

Disk diffusion plate assays were performed to test the sensitivity to the redox cycling compounds paraquat (5%) and menadione (80 mM) at a higher oxygen tension (cell to air interface). These assays were performed with both vegetative bacilli and purified spore preparations to differentiate the sensitivity of actively growing cells from the ability of dormant endospores to germinate and outgrow in an oxidatively stressful environment. Only the vegetative cells and spores of Δ*sodA1* are significantly more sensitive to paraquat and menadione than the parental Sterne strain and the other three Δ*sod* strains, showing significantly larger zones of inhibition (Fig. 5A to D). In addition, spores of Δ*sodA1* display an increased sensitivity to these compounds relative to replicating bacilli, suggesting that the amount of SODA1 present within the endospore is not sufficient for normal outgrowth under high oxidative stress. The Δ*sodA1* complemented strain [Δ*sodA1* (A1)] showed significantly smaller zones of inhibition compared to strains carrying an empty vector [Δ*sodA1*(pBJ258) and Sterne(pBJ258)] (Fig. 5E), although the zones of the complemented strain were not entirely reduced to the size of those for Sterne, suggesting that transcription from a low-copy plasmid provides partial complementation.

As mentioned above, *B. subtilis sodA* mutants display a striking spore morphology phenotype (23), and this particular SOD has been shown to be the main protective enzyme in *B. subtilis* from paraquat-induced oxidative stress (7). Of the four *B. anthracis* SODs, SODA1 shows the closest amino acid sequence homology (~77%) to the *B. subtilis* enzyme and also protects *B. anthracis* from intracellular superoxide stress. However, transmission electron microscopy of Δ*sodA1* mutants shows neither a change in average spore size nor any obvious morphological defect (not shown).

The results of bacterial growth under oxidatively stressful conditions both in broth and on plates confirm that, of the four SODs of *B. anthracis*, SODA1 protects against endogenously generated superoxide and therefore is the predominant protective enzyme during aerobic growth. It should also be noted that colonies of the Δ*sodA1* mutant on plates are generally smaller than those of parental Sterne and the other three Δ*sod* mutants, suggesting that at the agar-air interface, where oxygen tension is higher than in broth, SODA1 is needed for optimal growth.

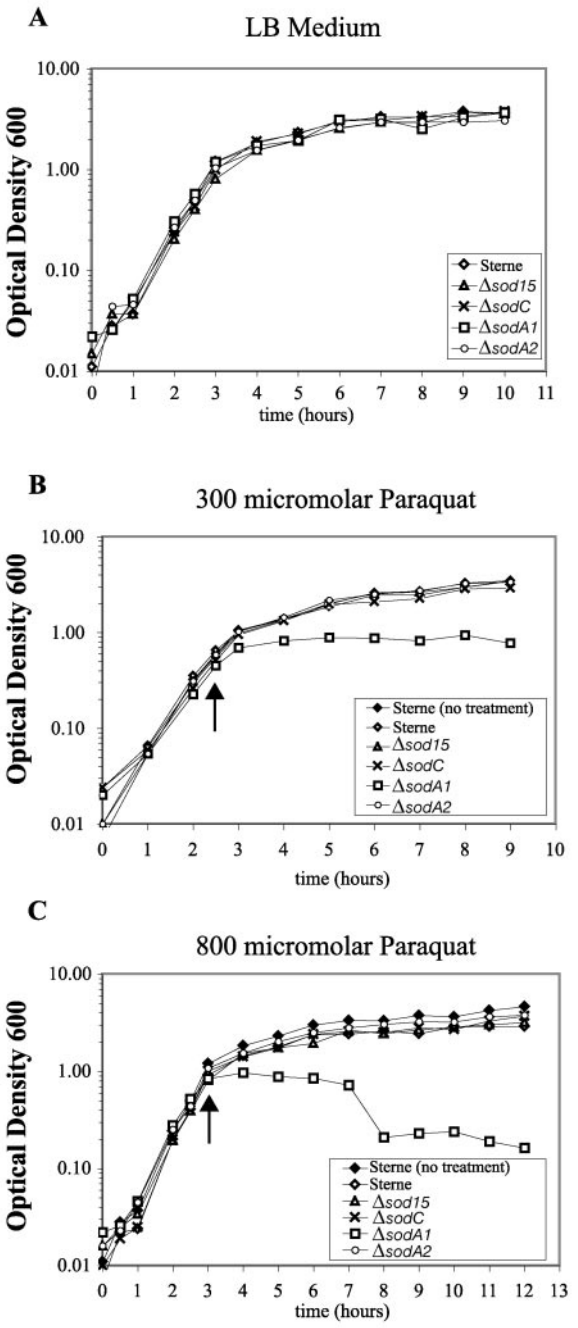

FIG. 4. Growth of Sterne and Δ*sod* strains in liquid broth under paraquat-induced superoxide stress. Arrows indicate the time at which paraquat was added to indicated concentration. (A) Growth of four Δ*sod* mutants is equivalent to the parental Sterne strain in liquid Luria-Bertani (LB) broth at 37°C. (B) Growth of Δ*sod* mutants in the presence of a low concentration of paraquat (300 μM) suggests that the lack of only one SOD protein is compensated for by the remaining paralogs; at a higher concentration (800 μM) (C), SODA1 is essential for survival into exponential phase, and a drop in OD_{600} suggests a lysis response. (The growth curves shown are representative of three independent experiments performed from three separate spore stocks all with the same trend.)

Intratracheal infections of mice with Δ*sod* mutants. The degree to which chromosomally encoded factors contribute to

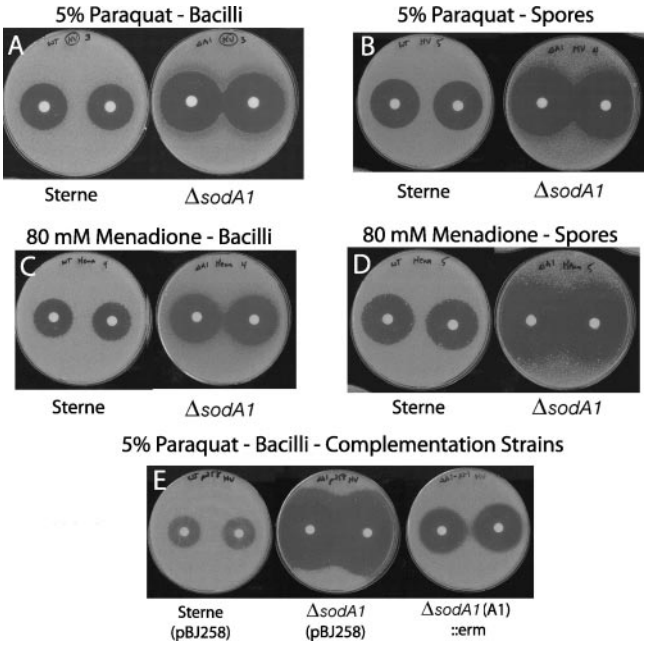

FIG. 5. Disk diffusion assays of the sensitivity of Δ*sod* mutants to the superoxide generating compounds paraquat and menadione. Photos are of plates from experiments listed in Table 3. Zones of inhibition of vegetative cells and spores from oxidative stress induced by 5% paraquat (A, B, and E) or 80 mM menadione (C and D). $n = 10$ disks per experiment.

the establishment of disease in *B. anthracis* is only now beginning to be addressed. To determine whether one of the four *B. anthracis* SODs is important for bacterial survival within a host, we performed survival studies on DBA/2 mice, a strain that is sensitive to infection with Sterne spores. The intratracheal route of infection was chosen to most closely mimic an inhalational route of spore entry. Table 4 indicates the LD_{50} determined for each strain in the present study, as well as final percent survivals and a mean times to death at an infectious dose of 10^4 spores. Experiments were also performed with 10^2, 10^3, and, for Sterne and the Δ*sodA1* mutant, 10^5 spores (not shown) to determine the LD_{50}s by the method of Reed and Muench (48). After 10 days, the percent survival values for

TABLE 4. LD_{50} and mean-time-to-death data for intratracheal infections of DBA/2 mice with 10^4 spores of *B. anthracis* Sterne and Δ*sod* mutants

Strain	LD_{50} (48)	% Survival	Mean days to death
Sterne ($34F_2$)	$\sim 4.5 \times 10^4$	22	2.4
Δ*sod15* mutant	$\sim 8.0 \times 10^4$	44	3.6
Δ*sodC* mutant	$\sim 5.0 \times 10^4$	25	3.0
Δ*sodA1* mutant	$\sim 1.0 \times 10^5$	56	2.4
Δ*sodA2* mutant	$\sim 5.0 \times 10^4$	33	2.3

mice infected with 10^4 spores of Sterne, Δ*sodC*, and Δ*sodA2* strains were similar: 22, 25, and 33%, respectively (Table 4). However, mice infected with an equivalent dose of Δ*sod15* and Δ*sodA1* showed higher rates of survival after 10 days, with 44 and 56% surviving, respectively. Log-rank tests performed on the stated data indicate *P* values of 0.4 for Δ*sod15* and 0.2 for Δ*sodA1*. These *P* values do not fall under the typical cutoff for statistical significance ($P \leq 0.05$) so, although the trends are very consistent, attenuation is only suggested. Interestingly, dissemination to the spleen was inconsistent for all strains; some of the dead and living mice had detectable bacterial loads in the spleen, and some did not. The lungs, however, all maintained a load of bacteria, both at the time of death and even in mice that had survived 10 days. Considering the complexity of modeling an inhalational route of infection via intratracheal delivery of spores and the lung environment in general, it does appear that the SOD15 and SODA1 may contribute slightly to bacterial fitness in a lung infection but are not essential for the microorganism to establish disease. Whether the Δ*sod15* and Δ*sodA1* mutants are slightly more sensitive to bacterial killing or are unable to grow efficiently at later time points is uncertain and is still under investigation.

DISCUSSION

Since the discovery of SOD in the 1960s (36), this important antioxidant enzyme has been characterized in numerous species, both eukaryotic and prokaryotic (2, 19, 38). The roles that SODs play in the disease-causing ability of pathogenic microorganisms are diverse, underlining the adaptability that prokaryotes have evolved to optimize growth in varied physical environments (see reference 34 for an excellent review). Two

TABLE 3. Disk diffusion assay of sensitivity to superoxide-generating compounds (with 6-mm paper disks)[a]

Compound	Zone of inhibition (diam) in mm ± SD				
	Sterne	Δ*sod15* mutant	Δ*sodC* mutant	Δ*sodA1* mutant	Δ*sodA2* mutant
Spores					
5% Methyl viologen	31.1 ± 0.7	31.6 ± 0.5	30.8 ± 0.4	42.6 ± 0.8*	31.0 ± 1.1
80 mM menadione	31.4 ± 0.7	30.6 ± 0.5	30.4 ± 0.5	49.1 ± 1.0*	31.6 ± 0.7
Bacilli					
5% Methyl viologen	27.1 ± 0.6	27.5 ± 0.7	26.9 ± 0.6	38.3 ± 1.6*	27.4 ± 0.5
80 mM menadione	24.4 ± 0.5	24.0 ± 0.5	24.8 ± 0.4	32.6 ± 1.1*	26.1 ± 0.6
	Sterne + pBJ258	Δ*sodA1* + pBJ258	Δ*sodA1*(*A1*) + *sodA1*	Δ*sodA2* + pBJ258	Δ*sodA2*(*A2*) + *sodA2*
Bacilli (complementation strains)					
5% Methyl viologen	24.4 ± 1.0	56.7 ± 1.6	34.1 ± 1.0**	26.1 ± 1.0	24.9 ± 1.2

[a] *, $P \leq 0.001$ (different from wild type; two-tailed *t* test); **, $P \leq 0.001$ (different from wild-type, original strain, and original strain with plasmid alone; two-tailed *t* test). $n = 10$ disks per compound (two disks per BHI plate). All H_2O controls: zones = 0 mm.

of the four encoded putative SODs of *B. anthracis*, SOD15 and SODA1, were found to be resident proteins of the endospore, the infectious form of this microorganism (33). In this proteomic analysis, SOD15 was identified in the soluble, membrane, and exosporium fractions, whereas SODA1 was eluted in the soluble and exosporium fractions. It should be noted, however, that the exosporium fractions in the present study most likely also contained some proteins from the spore coat; therefore, the exact location of these two enzymes in the spore is still not entirely clear. In addition, *B. anthracis* carries two other putative *sod* genes on the genome (*sodA2* and *sodC*). The quantity and diversity of the encoded SODs prompted us to create single-deletion mutants in each of the four *B. anthracis sod* genes to determine whether these proteins work cooperatively as antioxidants or whether they might have unique functions in different growth environments.

Only *sod15* shows a transcriptional profile that suggests some form of adaptive regulation, where mRNA abundance is low during exponential growth but increases dramatically during the late exponential and sporulation phases. However, although the other *sod* genes displayed constitutive expression under our experimental conditions, they may, indeed, be differentially regulated under conditions different from those tested here such as, for example, under alternative stresses or during infection. The transcriptional profile of *sod15* suggests that it may be a member of a stress-induced regulon, since entry into sporulation phase is initiated by signals such as DNA damage and nutrient depletion (56). Its transcription at high OD_{600} as part of a four-gene operon that includes homologs to *B. subtilis* genes that are important for the formation of normal endospores (*dacB* operon) (43) suggests that *sod15* may have a minor role in the formation of spores. *B. subtilis* cells lacking *sodA* or the *dacB* operon have strong spore structure defects (23, 43). Electron microscopy of *B. anthracis* Δ*sod15* mutant spores reveals only minor, sporadic differences in spore ultrastructure. Also, Δ*sod15* spores do not have a germination defect as measured by a drop in the OD_{600} in 100 mM L-alanine compared to the parental Sterne strain. This differs from the radical phenotypes of *B. subtilis dacB* and *sodA* mutants. Henriques et al. (23) suggest that the role SOD could play in *B. subtilis* spore formation is indirectly catalytic, changing the oxidative microenvironment during coat assembly and facilitating dityrosine linkages of coat proteins. However, the only biochemical precedent describing a similar phenomenon is in eukaryotes (32, 58) and has not yet been substantiated in prokaryotes. Further in vitro biochemical analysis with recombinant proteins may aid in explaining why *sod15* is part of an operon putatively involved in cell morphology. Since Δ*sod15* strain causes slightly less mortality in intratracheal infections of mice, it is possible that spore integrity is compromised in a way that is not visible at the ultrastructure level.

The Δ*sodA1* strain consistently revealed a major phenotype in terms of sensitivity to endogenous superoxide stress. During exponential growth and entry into the stationary or sporulation phase in sporulation medium, the transcriptional levels of *sodA1* are consistently the highest of the four *sod* genes, whereas *sodA2* shows the lowest abundance of transcript, further supporting a leading role for the *sodA1* paralog. Growth under intracellular superoxide stress induced in vitro, both in broth (300 and 800 μM paraquat) and on agar plates (paraquat and menadione), shows that SODA1 is an extremely important enzyme for protection from endogenously generated superoxide stress. Also, spores of this strain are even more sensitive to a strongly oxidative environment than replicating bacilli, suggesting that the amount of SOD in the spore is important for efficient outgrowth under high oxidative stress. Of the four *B. anthracis* SODs, SODA1 shares the highest amino acid identity with *B. subtilis* SODA, but differences in spore ultrastructure were not apparent in the Δ*sodA1* mutant strain by transmission electron microscopy, again underlining differences in the role of SODs in these two species. In mouse intratracheal infections, the Δ*sodA1* strain caused less mortality than the parental Sterne strain, although not within a statistically significant range. A recent study of the ability of neutrophils to kill *B. anthracis* (35) suggests that, at least in these phagocytes, killing is independent of the oxidative burst, since cells treated with the NADPH oxidase inhibitor DPI were just as efficient at killing as those without treatment, suggesting that *B. anthracis* SODs may not be strongly protective from the host oxidative burst. Because Δ*sodA1* mutants struggle in the presence of intracellular superoxide, *sodA1* most likely serves *B. anthracis* by protecting it from metabolically generated oxidative stress during rapid growth during infection and in vitro growth.

The crystal structures of SODA1 and SODA2 were recently determined as homodimers with chelated Mn as the catalytic metal (4). Our nondenaturing PAGE-nitroblue tetrazolium SOD activity assays of Δ*sod* mutants and complemented strains strongly suggest that SODA1 and SODA2 form both homodimers and heterodimers. The possibility that one or both of these enzymes might be able to utilize Fe as a catalytic metal has not been tested. Since the Δ*sodA2* mutant is not sensitive to superoxide stress and is able to cause the same amount of mortality in mouse intratracheal infections as parental Sterne, it is unclear how important this gene or the A1/A2 heterodimer form of the enzyme is for normal growth. A possible level of redundancy that might exist between the four putative SODs may not be apparent in the phenotypes of single mutants but could be apparent in multiple knockouts.

In conclusion, our initial survey of the four *B. anthracis* SODs shows *sodA1* to be the prototypical, cellular antioxidant enzyme needed for growth under endogenously generated superoxide stress. *sod15*, on the other hand, may or may not actually function as a SOD in vivo, but its presence in the endospore, its conservation in the *B. cereus* group, and its unusual transcriptional pattern as part of an operon putatively involved in cell morphology make this an intriguing target for future biochemical characterization. The role of *sodA2*, which has been functionally isolated from both endospores and vegetative cells and which most likely forms an active heterodimer with *sodA1*, may serve a minor role in cellular antioxidant protection that is not apparent in single deletion strains. The removal of *sodC* did not evoke an obvious phenotype in any of the assays performed here, even though this gene is actively transcribed in wild-type cells. *B. anthracis* encodes multiple antioxidant enzyme systems, such as catalases and peroxidases, underlining the complex defense strategies that this important pathogen has evolved to cope with variably generated oxidative stresses.

ACKNOWLEDGMENTS

Special thanks go to Brian Janes, Dotty Sorenson (University of Michigan Microscopy and Imaging Lab), Joe Washburn (University of Michigan cDNA Core), and Rod McDonald for all manner of technical assistance.

Funding for this project was provided in part by the NIH-funded Cellular Biotechnology Training Program at the University of Michigan. This study was also supported in part by HHS contract N266200400059C/N01-AI-40059, by NIH grant AI08649, and by the Great Lakes and the Southeast Regional Centers of Excellence for Biodefense and Emerging Infections.

REFERENCES

1. **Banci, L., I. Bertini, V. Calderone, F. Cramaro, R. Del Conte, A. Fantoni, S. Mangani, A. Quattrone, and M. S. Viezzoli.** 2005. A prokaryotic superoxide dismutase paralog lacking two Cu ligands: from largely unstructured in solution to ordered in the crystal. Proc. Natl. Acad. Sci. USA **102:**7541–7546.
2. **Battistoni, A.** 2003. Role of prokaryotic Cu,Zn superoxide dismutase in pathogenesis. Biochem. Soc. Trans. **31:**1326–1329.
3. **Beyer, W., J. Imlay, and I. Fridovich.** 1991. Superoxide dismutases. Prog. Nucleic Acids Res. Mol. Biol. **40:**221–253.
4. **Boucher, I. W. K. A., V. M. Levdikov, E. V. Blagova, M. J. Fogg, J. A. Brannigan, K. S. Wilson, and A. J. Wilkinson.** 2005. Structures of two superoxide dismutases from *Bacillus anthracis* reveal a novel active center. Acta Crystallogr. Sect. F Struct. Biol. Crystal. Commun. **2005:**621–624.
5. **Braunstein, M., B. J. Espinosa, J. Chan, J. T. Belisle, and W. R. Jacobs, Jr.** 2003. SecA2 functions in the secretion of superoxide dismutase A and in the virulence of *Mycobacterium tuberculosis*. Mol. Microbiol. **48:**453–464.
6. **Brioukhanov, A. L., and A. I. Netrusov.** 2004. Catalase and superoxide dismutase: distribution, properties, and physiological role in cells of strict anaerobes. Biochemistry **69:**949–962.
7. **Casillas-Martinez, L., and P. Setlow.** 1997. Alkyl hydroperoxide reductase, catalase, MrgA, and superoxide dismutase are not involved in resistance of *Bacillus subtilis* spores to heat or oxidizing agents. J. Bacteriol. **179:**7420–7425.
8. **Cendrowski, S., W. MacArthur, and P. Hanna.** 2004. *Bacillus anthracis* requires siderophore biosynthesis for growth in macrophages and mouse virulence. Mol. Microbiol. **51:**407–417.
9. **De Groote, M. A., U. A. Ochsner, M. U. Shiloh, C. Nathan, J. M. McCord, M. C. Dinauer, S. J. Libby, A. Vazquez-Torres, Y. Xu, and F. C. Fang.** 1997. Periplasmic superoxide dismutase protects *Salmonella* from products of phagocyte NADPH-oxidase and nitric oxide synthase. Proc. Natl. Acad. Sci. USA **94:**13997–14001.
10. **Dixon, T. C., M. Meselson, J. Guillemin, and P. C. Hanna.** 1999. Anthrax. N. Engl. J. Med. **341:**815–826.
11. **Drysdale, M., S. Heninger, J. Hutt, Y. Chen, C. R. Lyons, and T. M. Koehler.** 2005. Capsule synthesis by *Bacillus anthracis* is required for dissemination in murine inhalation anthrax. EMBO J. **24:**221–227.
12. **Dussurget, O., G. Stewart, O. Neyrolles, P. Pescher, D. Young, and G. Marchal.** 2001. Role of *Mycobacterium tuberculosis* copper-zinc superoxide dismutase. Infect. Immun. **69:**529–533.
13. **Eberhardt, M. K.** 2001. Reactive oxygen metabolites: chemistry and medical consequences. CRC Press, Boca Raton, Fla.
14. **Edwards, K. M., M. H. Cynamon, R. K. Voladri, C. C. Hager, M. S. DeStefano, K. T. Tham, D. L. Lakey, M. R. Bochan, and D. S. Kernodle.** 2001. Iron-cofactored superoxide dismutase inhibits host responses to *Mycobacterium tuberculosis*. Am. J. Respir. Crit. Care Med. **164:**2213–2219.
15. **Fang, F. C., M. A. DeGroote, J. W. Foster, A. J. Baumler, U. Ochsner, T. Testerman, S. Bearson, J. C. Giard, Y. Xu, G. Campbell, and T. Laessig.** 1999. Virulent *Salmonella typhimurium* has two periplasmic Cu, Zn-superoxide dismutases. Proc. Natl. Acad. Sci. USA **96:**7502–7507.
16. **Farrant, J. L., A. Sansone, J. R. Canvin, M. J. Pallen, P. R. Langford, T. S. Wallis, G. Dougan, and J. S. Kroll.** 1997. Bacterial copper- and zinc-cofactored superoxide dismutase contributes to the pathogenesis of systemic salmonellosis. Mol. Microbiol. **25:**785–796.
17. **Fisher, N., and P. Hanna.** 2005. Characterization of *Bacillus anthracis* germinant receptors in vitro. J. Bacteriol. **187:**8055–8062.
18. **Franzon, V. L., J. Arondel, and P. J. Sansonetti.** 1990. Contribution of superoxide dismutase and catalase activities to *Shigella flexneri* pathogenesis. Infect. Immun. **58:**529–535.
19. **Frealle, E., C. Noel, E. Viscogliosi, D. Camus, E. Dei-Cas, and L. Delhaes.** 2005. Manganese superoxide dismutase in pathogenic fungi: an issue with pathophysiological and phylogenetic involvements. FEMS Immunol. Med. Microbiol. **45:**411–422.
20. **Guarner, J., J. A. Jernigan, W. J. Shieh, K. Tatti, L. M. Flannagan, D. S. Stephens, T. Popovic, D. A. Ashford, B. A. Perkins, and S. R. Zaki.** 2003. Pathology and pathogenesis of bioterrorism-related inhalational anthrax. Am. J. Pathol. **163:**701–709.
21. **Guerout-Fleury, A. M., K. Shazand, N. Frandsen, and P. Stragier** 1995. Antibiotic-resistance cassettes for *Bacillus subtilis*. Gene **167:**335–336.
22. **Gusarov, I., and E. Nudler.** 2005. NO-mediated cytoprotection: instant adaptation to oxidative stress in bacteria. Proc. Natl. Acad. Sci. USA **102:**13855–13860.
23. **Henriques, A. O., L. R. Melsen, and C. P. Moran, Jr.** 1998. Involvement of superoxide dismutase in spore coat assembly in *Bacillus subtilis*. J. Bacteriol. **180:**2285–2291.
24. **Heyworth, P. G., A. R. Cross, and J. T. Curnutte.** 2003. Chronic granulomatous disease. Curr. Opin. Immunol. **15:**578–584.
25. **Imlay, J.** 2006. Iron-sulphur clusters and the problem with oxygen. Mol. Microbiol. **59:**1073–1082.
26. **Imlay, J. A.** 2003. Pathways of oxidative damage. Annu. Rev. Microbiol. **57:**395–418.
27. **Inaoka, T., Y. Matsumura, and T. Tsuchido.** 1998. Molecular cloning and nucleotide sequence of the superoxide dismutase gene and characterization of its product from *Bacillus subtilis*. J. Bacteriol. **180:**3697–3703.
28. **Jackson, S. M., and J. B. Cooper.** 1998. An analysis of structural similarity in the iron and manganese superoxide dismutases based on known structures and sequences. Biometals **11:**159–173.
29. **Keyer, K., and J. A. Imlay.** 1996. Superoxide accelerates DNA damage by elevating free-iron levels. Proc. Natl. Acad. Sci. USA **93:**13635–13640.
30. **Kroll, J. S., P. R. Langford, K. E. Wilks, and A. D. Keil.** 1995. Bacterial [Cu,Zn]-superoxide dismutase: phylogenetically distinct from the eukaryotic enzyme, and not so rare after all! Microbiology **141**(Pt. 9)**:**2271–2279.
31. **Lai, E. M., N. D. Phadke, M. T. Kachman, R. Giorno, S. Vazquez, J. A. Vazquez, J. R. Maddock, and A. Driks.** 2003. Proteomic analysis of the spore coats of *Bacillus subtilis* and *Bacillus anthracis*. J. Bacteriol. **185:**1443–1454.
32. **Larios, J. M., R. Budhiraja, B. L. Fanburg, and V. J. Thannickal.** 2001. Oxidative protein cross-linking reactions involving L-tyrosine in transforming growth factor-β1-stimulated fibroblasts. J. Biol. Chem. **276:**17437–17441.
33. **Liu, H., N. H. Bergman, B. Thomason, S. Shallom, A. Hazen, J. Crossno, D. A. Rasko, J. Ravel, T. D. Read, S. N. Peterson, J. Yates III, and P. C. Hanna.** 2004. Formation and composition of the *Bacillus anthracis* endospore. J. Bacteriol. **186:**164–178.
34. **Lynch, M., and H. Kuramitsu.** 2000. Expression and role of superoxide dismutases (SOD) in pathogenic bacteria. Microbes Infect. **2:**1245–1255.
35. **Mayer-Scholl, A., R. Hurwitz, V. Brinkmann, M. Schmid, P. Jungblut, Y. Weinrauch, and A. Zychlinsky.** 2005. Human neutrophils kill *Bacillus anthracis*. PLoS Pathog. **1:**e2.
36. **McCord, J. M., and I. Fridovich.** 1969. Superoxide dismutase. An enzymic function for erythrocuprein (hemocuprein). J. Biol. Chem. **244:**6049–6055.
37. **Munoz-Montesino, C., E. Andrews, R. Rivers, A. Gonzalez-Smith, G. Moraga-Cid, H. Folch, S. Cespedes, and A. A. Onate.** 2004. Intraspleen delivery of a DNA vaccine coding for superoxide dismutase (SOD) of *Brucella abortus* induces SOD-specific $CD4^+$ and $CD8^+$ T cells. Infect. Immun. **72:**2081–2087.
38. **Nozik-Grayck, E., H. B. Suliman, and C. A. Piantadosi.** 2005. Extracellular superoxide dismutase. Int. J. Biochem. Cell. Biol. **37:**2466–2471.
39. **Parker, M. W., and C. C. Blake.** 1988. Iron- and manganese-containing superoxide dismutases can be distinguished by analysis of their primary structures. FEBS Lett. **229:**377–382.
40. **Parker, M. W., C. C. Blake, D. Barra, F. Bossa, M. E. Schinina, W. H. Bannister, and J. V. Bannister.** 1987. Structural identity between the iron- and manganese-containing superoxide dismutases. Protein Eng. **1:**393–397.
41. **Piddington, D. L., F. C. Fang, T. Laessig, A. M. Cooper, I. M. Orme, and N. A. Buchmeier.** 2001. Cu,Zn superoxide dismutase of *Mycobacterium tuberculosis* contributes to survival in activated macrophages that are generating an oxidative burst. Infect. Immun. **69:**4980–4987.
42. **Pollock, J. D., D. A. Williams, M. A. Gifford, L. L. Li, X. Du, J. Fisherman, S. H. Orkin, C. M. Doerschuk, and M. C. Dinauer.** 1995. Mouse model of X-linked chronic granulomatous disease, an inherited defect in phagocyte superoxide production. Nat. Genet. **9:**202–209.
43. **Popham, D. L., B. Illades-Aguiar, and P. Setlow.** 1995. The *Bacillus subtilis dacB* gene, encoding penicillin-binding protein 5*, is part of a three-gene operon required for proper spore cortex synthesis and spore core dehydration. J. Bacteriol. **177:**4721–4729.
44. **Poyart, C., E. Pellegrini, O. Gaillot, C. Boumaila, M. Baptista, and P. Trieu-Cuot.** 2001. Contribution of Mn-cofactored superoxide dismutase (SodA) to the virulence of *Streptococcus agalactiae*. Infect. Immun. **69:**5098–5106.
45. **Quinn, C. P., and B. N. Dancer.** 1990. Transformation of vegetative cells of *Bacillus anthracis* with plasmid DNA. J. Gen. Microbiol. **136:**1211–1215.
46. **Rainey, G. J., D. J. Wigelsworth, P. L. Ryan, H. M. Scobie, R. J. Collier, and J. A. Young.** 2005. Receptor-specific requirements for anthrax toxin delivery into cells. Proc. Natl. Acad. Sci. USA **102:**13278–13283.
47. **Read, T. D., S. N. Peterson, N. Tourasse, L. W. Baillie, I. T. Paulsen, K. E. Nelson, H. Tettelin, D. E. Fouts, J. A. Eisen, S. R. Gill, E. K. Holtzapple, O. A. Okstad, E. Helgason, J. Rilstone, M. Wu, J. F. Kolonay, M. J. Beanan, R. J. Dodson, L. M. Brinkac, M. Gwinn, R. T. DeBoy, R. Madpu, S. C. Daugherty, A. S. Durkin, D. H. Haft, W. C. Nelson, J. D. Peterson, M. Pop, H. M. Khouri, D. Radune, J. L. Benton, Y. Mahamoud, L. Jiang, I. R. Hance, J. F. Weidman, K. J. Berry, R. D. Plaut, A. M. Wolf, K. L. Watkins, W. C. Nierman, A. Hazen, R. Cline, C. Redmond, J. E. Thwaite, O. White, S. L.**

Salzberg, B. Thomason, A. M. Friedlander, T. M. Koehler, P. C. Hanna, A. B. Kolsto, and C. M. Fraser. 2003. The genome sequence of *Bacillus anthracis* Ames and comparison to closely related bacteria. Nature **423:**81–86.

48. **Reed, L. J., and H. Muench.** 1938. A simple method of estimating fifty per cent endpoints. Am. J. Hyg. **27:**493–497.
49. **Reeves, E. P., H. Lu, H. L. Jacobs, C. G. Messina, S. Bolsover, G. Gabella, E. O. Potma, A. Warley, J. Roes, and A. W. Segal.** 2002. Killing activity of neutrophils is mediated through activation of proteases by K^+ flux. Nature **416:**291–297.
50. **Reeves, E. P., M. Nagl, J. Godovac-Zimmermann, and A. W. Segal.** 2003. Reassessment of the microbicidal activity of reactive oxygen species and hypochlorous acid with reference to the phagocytic vacuole of the neutrophil granulocyte. J. Med. Microbiol. **52:**643–651.
51. **Ruthel, G., W. J. Ribot, S. Bavari, and T. A. Hoover.** 2004. Time-lapse confocal imaging of development of *Bacillus anthracis* in macrophages. J. Infect. Dis. **189:**1313–1316.
52. **Smith, K., and P. Youngman.** 1992. Use of a new integrational vector to investigate compartment-specific expression of the *Bacillus subtilis* spoIIM gene. Biochimie **74:**705–711.
53. **Spagnolo, L., I. Toro, M. D'Orazio, P. O'Neill, J. Z. Pedersen, O. Carugo, G. Rotilio, A. Battistoni, and K. Djinovic-Carugo.** 2004. Unique features of the *sodC*-encoded superoxide dismutase from *Mycobacterium tuberculosis*, a fully functional copper-containing enzyme lacking zinc in the active site. J. Biol. Chem. **279:**33447–33455.
54. **Storz, G., and R. Hengge-Aronis.** 2000. Bacterial stress responses. ASM Press, Washington, D.C.
55. **Storz, G., and J. A. Imlay.** 1999. Oxidative stress. Curr. Opin. Microbiol. **2:**188–194.
56. **Stragier, P., and R. Losick.** 1996. Molecular genetics of sporulation in *Bacillus subtilis*. Annu. Rev. Genet. **30:**297–341.
57. **Sutton, V. R., A. Stubna, T. Patschkowski, E. Munck, H. Beinert, and P. J. Kiley.** 2004. Superoxide destroys the $[2Fe\text{-}2S]^{2+}$ cluster of FNR from *Escherichia coli*. Biochemistry **43:**791–798.
58. **Thannickal, V. J.** 2003. The paradox of reactive oxygen species: injury, signaling, or both? Am. J. Physiol. Lung Cell Mol. Physiol. **284:**L24–L25.
59. **Tsolis, R. M., A. J. Baumler, and F. Heffron.** 1995. Role of *Salmonella typhimurium* Mn-superoxide dismutase (SodA) in protection against early killing by J774 macrophages. Infect. Immun. **63:**1739–1744.